Fourier-matching Pseudospectral Modal Method for Diffraction Gratings

Dawei Song[1,2], Lijun Yuan[2] and Ya Yan Lu[2]

[1]*Department of Mathematics, University of Science and Technology of China Hefei, Anhui, China*

[2]*Department of Mathematics, City University of Hong Kong Kowloon, Hong Kong*

A Fourier-matching pseudospectral modal method (PSMM(f)) is developed for analyzing lamellar diffraction gratings or grating stacks. A Chebyshev pseudospectral method is first used to accurately calculate the eigenmodes of the grating layers, and then the Fourier coefficients are matched at the interfaces between the layers. Compared with an existing pseudospectral modal method based on point-matching, the PSMM(f) is more robust and accurate. The method performs better than the standard Fourier modal method for gratings involving metals.

OCIS codes: 050.1950, 000.4430

1. Introduction

In the past several decades, many numerical methods have been developed for analyzing diffraction gratings and other periodic structures. For lamellar gratings or multilayer lamellar grating stacks, analytic and numerical modal methods are very natural and widely used. The analytic modal method (AMM) [1–10] expresses the eigenmodes of the grating layer analytically in each homogeneous segment and solves the propagation constants of the modes from a transcendental equation. Numerical modal methods include the Fourier modal method (FMM) [11–21], a Legendre/Chebyshev polynomial expansion modal method (PEMM) [22], a finite difference modal method (FDMM) [23] and a B-spline modal method [24, 25], a point-matching pseudospectral modal method (PSMM(p)) [26], etc. For diffraction gratings involving metals or other lossy media, the propagation constants of the eigenmodes are complex in general. In that case, the AMM requires sophisticated techniques to systematically find complex solutions of a transcendental equation [3]. This can be somewhat complicated, especially for grating layers with more than two homogeneous segments [8]. Numerical modal methods are easier to use, since the eigenmodes are simply calculated from approximate matrix eigenvalue problems. Due to its simplicity, the FMM is extremely popular. However,

for highly conducting gratings, the standard implementation of FMM has some convergence problems. A number of techniques have been proposed to address this issue [18, 20, 21]. The other numerical modal methods, such as the FDMM [23], may have some advantages for analyzing metallic gratings. On the other hand, the FMM has been enhanced by the adaptive spatial resolution technique [17]. Despite of the many improvements, the FMM and other numerical modal methods still cannot compete with a properly implemented AMM [9, 10]. Therefore, it is still desirable to develop new numerical modal methods which are simple to implement and perform more like the AMM.

For both the PEMM [22] and the PSMM(p) [26], the eigenfunctions are approximated by piecewise polynomials. The difference is that the PEMM works with the expansion coefficients, while the PSMM(p) uses the notion of differentiation matrices and works in the physical space. As a consequence, the PEMM given in [22] is only valid for grating layers with piecewise constant refractive index profiles, while the PSMM(p) is applicable to structures with graded index distributions, although the implementation in [26] is only for piecewise constant profiles. In this paper, we present a Fourier-matching pseudospectral modal method (PSMM(f)) for lamellar gratings and lamellar grating stacks. Unlike the PSMM(p) given in [26] where the interface conditions between the different layers are implemented by a point-matching scheme, we approximate the interface conditions by matching Fourier coefficients as in the FMM. Furthermore, we use only a portion of the numerical eigenmodes, since some of the higher order modes are numerical artifacts unrelated to any physical modes. A least squares technique developed in [20, 21] is also incorporated into our method for producing more reliable solutions for certain cases.

2. Basic formulation

We consider one-dimensional (1D) gratings which are invariant in z and periodic in x with period L, where $\{x, y, z\}$ is a Cartesian coordinate system. For the transverse magnetic (TM) polarization, the z component of the magnetic field, denoted by u in this paper, is the only non-zero component of the magnetic field, and it satisfies the following Helmholtz equation

$$\frac{\partial}{\partial x}\left(\frac{1}{\varepsilon}\frac{\partial u}{\partial x}\right) + \frac{\partial}{\partial y}\left(\frac{1}{\varepsilon}\frac{\partial u}{\partial y}\right) + k_0^2 \mu\, u = 0, \tag{1}$$

where k_0 is the free space wavenumber, ε and μ are the relative permittivity (dielectric constant) and relative permeability of the media, respectively. For the transverse electric (TE) polarization, the governing equation is for the z component of the electric field and it can be obtained by exchanging μ and ε in Eq. (1). The grating layer or stack is assumed to be given by $0 < y < D$ where D is a constant, so that ε and μ are constants $\{\varepsilon^{(0)}, \mu^{(0)}\}$ for $y < 0$ and $\{\varepsilon^{(*)}, \mu^{(*)}\}$ for $y > D$. Furthermore, we assume that the grating structure is piecewise uniform in y and the uniform layers are separated by $0 = y_0 < y_1 < y_2 < ... < y_J = D$,

where J is the total number of layers. In each layer, ε and μ are functions of x only, i.e.,

$$\varepsilon(x,y) = \varepsilon^{(j)}(x), \quad \mu(x,y) = \mu^{(j)}(x), \quad y_{j-1} < y < y_j. \tag{2}$$

In the top region ($y > D$), we specify a plane incident wave

$$u^{(i)} = \exp\{i[\alpha_0 x - \beta_0^{(*)}(y-D)]\}, \quad y > D. \tag{3}$$

If the angle of incidence between the incident wave vector and the y-axis is θ, then

$$\alpha_0 = k_0\sqrt{\varepsilon^{(*)}\mu^{(*)}}\sin\theta, \quad \beta_0^{(*)} = k_0\sqrt{\varepsilon^{(*)}\mu^{(*)}}\cos\theta.$$

The incident wave gives rise to a reflected wave $u^{(r)}$ in the top and a transmitted wave $u^{(t)}$ in the bottom ($y < 0$), and they have the following expansions:

$$u^{(r)}(x,y) = \sum_{m=-\infty}^{\infty} R_m \exp\{i[\alpha_m x + \beta_m^{(*)}(y-D)]\}, \quad y > D, \tag{4}$$

$$u^{(t)}(x,y) = \sum_{m=-\infty}^{\infty} T_m \exp[i(\alpha_m x - \beta_m^{(0)} y)], \quad y < 0, \tag{5}$$

where

$$\alpha_m = \alpha_0 + \frac{2\pi m}{L}, \quad \beta_m^{(0)} = \sqrt{k_0^2\varepsilon^{(0)}\mu^{(0)} - \alpha_m^2}, \quad \beta_m^{(*)} = \sqrt{k_0^2\varepsilon^{(*)}\mu^{(*)} - \alpha_m^2}, \tag{6}$$

R_m and T_m are the reflection and transmission amplitudes to be determined.

In each layer, we expand the solution in the eigenmodes, that is

$$u(x,y) = \sum_{l=1}^{\infty} \left\{ a_l^{(j)} \exp[i\beta_l^{(j)}(y - y_{j-1})] + b_l^{(j)} \exp[i\beta_l^{(j)}(y_j - y)] \right\} g_l^{(j)}(x) \tag{7}$$

for $y_{j-1} < y < y_j$, where $\beta_l^{(j)}$ (more precisely its square) and $g_l^{(j)}$ are the lth eigenvalue and the corresponding eigenfunction in the jth layer. The eigenpair $\{g_l^{(j)}, \beta_l^{(j)}\}$ satisfies the following eigenvalue problem

$$\varepsilon \frac{d}{dx}\left(\frac{1}{\varepsilon}\frac{dg}{dx}\right) + k_0^2\varepsilon\mu\, g = \beta^2\, g, \quad 0 < x < L, \tag{8}$$

$$g(L) = e^{i\alpha_0 L} g(0), \tag{9}$$

$$\frac{1}{\varepsilon(L^-)}\frac{dg}{dx}(L^-) = \frac{e^{i\alpha_0 L}}{\varepsilon(0^+)}\frac{dg}{dx}(0^+). \tag{10}$$

To simplify the notations, we have dropped the subscript (j) for ε, μ, g and β, and the subscript l for g and β in the above equations. To solve the coefficients $a_l^{(j)}$, $b_l^{(j)}$, R_m and T_m, we need to set up a system of equations from the following continuity conditions

$$u(x, y_j^-) = u(x, y_j^+), \quad \frac{1}{\varepsilon(x,y_j^-)}\frac{\partial u}{\partial y}(x,y_j^-) = \frac{1}{\varepsilon(x,y_j^+)}\frac{\partial u}{\partial y}(x,y_j^+) \tag{11}$$

for $j = 0, 1, 2, ..., J$. Different modal methods correspond to different methods used to solve the eigenvalue problem (8-10) and impose the continuity conditions (11) approximately.

3. Computing the eigenmodes

In [26], a pseudospectral method for solving the eigenvalue problem (8-10) is given for the special case where one period of the grating contains two segments and each segment has a constant ε and μ. In the following, we present the pseudospectral method for the general case where ε and μ are piecewise smooth functions of x. We assume that the discontinuities of ε or μ are located at $0 = x_0 < x_1 < ... < x_P = L$, where L is the period in the x direction and P is the number of segments in the y-independent layer.

For the pth segment given by $x_{p-1} < x < x_p$, we discretize x by $q_p + 1$ points as

$$\xi_{p,k} = x_{p-1} + \frac{x_p - x_{p-1}}{2}\left[1 - \cos\left(\frac{k\pi}{q_p}\right)\right], \quad 0 \le k \le q_p. \tag{12}$$

Notice that $\xi_{p,0} = x_{p-1}$ and $\xi_{p,q_p} = x_p$. The Chebyshev pseudospectral method (also called Chebyshev collocation method) [27] approximates the first order derivative by a differentiation matrix $\mathbf{C}^{(p)}$ such that

$$\begin{bmatrix} g'(x_{p-1}^+) \\ \mathbf{g}'_p \\ g'(x_p^-) \end{bmatrix} \approx \mathbf{C}^{(p)} \begin{bmatrix} g(x_{p-1}) \\ \mathbf{g}_p \\ g(x_p) \end{bmatrix}, \tag{13}$$

where $\mathbf{g}_p$ is the column vector of g at the interior discretization points, i.e.,

$$\mathbf{g}_p = \Big[g(\xi_{p,1}), \quad g(\xi_{p,2}), \quad ..., \quad g(\xi_{p,q_p-1})\Big]^T, \tag{14}$$

and the prime denotes the derivative with respect to x. The entries of $\mathbf{C}^{(p)}$ are

$$C_{kl}^{(p)} = -\frac{2}{x_p - x_{p-1}} \begin{cases} (2q_p^2+1)/6 & \text{if } \ k = l = 0, \\ -(2q_p^2+1)/6 & \text{if } \ k = l = q_p, \\ -0.5\gamma_k/(1-\gamma_k^2) & \text{if } \ 0 < k = l < q_p, \\ (-1)^{k+l}\sigma_k\sigma_l^{-1}/(\gamma_k - \gamma_l) & \text{otherwise,} \end{cases}$$

where $\sigma_0 = \sigma_{q_p} = 2$, $\sigma_k = 1$ and $\gamma_k = \cos(k\pi/q_p)$ for $0 < k < q_p$. Let us write down the matrix $\mathbf{C}^{(p)}$ as

$$\mathbf{C}^{(p)} = \begin{bmatrix} c_1^{(p)} & \mathbf{c}_2^{(p)} & c_3^{(p)} \\ \mathbf{c}_4^{(p)} & \mathbf{C}_5^{(p)} & \mathbf{c}_6^{(p)} \\ c_7^{(p)} & \mathbf{c}_8^{(p)} & c_9^{(p)} \end{bmatrix}, \tag{15}$$

where $c_1^{(p)}$, $c_3^{(p)}$, $c_7^{(p)}$ and $c_9^{(p)}$ are the four corner entries of $\mathbf{C}^{(p)}$, $\mathbf{c}_2^{(p)}$ and $\mathbf{c}_8^{(p)}$ are row vectors of length $q_p - 1$, $\mathbf{c}_4^{(p)}$ and $\mathbf{c}_6^{(p)}$ are column vectors of length $q_p - 1$, $\mathbf{C}_5^{(p)}$ is a $(q_p - 1) \times (q_p - 1)$ matrix. This leads to

$$g'(x_{p-1}^+) \approx c_1^{(p)}\, g(x_{p-1}) + \mathbf{c}_2^{(p)}\, \mathbf{g}_p + c_3^{(p)} g(x_p), \tag{16}$$

$$\mathbf{g}'_p \approx \mathbf{c}_4^{(p)}\, g(x_{p-1}) + \mathbf{C}_5^{(p)}\, \mathbf{g}_p + \mathbf{c}_6^{(p)} g(x_p), \tag{17}$$

$$g'(x_p^-) \approx c_7^{(p)}\, g(x_{p-1}) + \mathbf{c}_8^{(p)}\, \mathbf{g}_p + c_9^{(p)} g(x_p). \tag{18}$$

For an interior discontinuity point x_p, $1 \le p \le P-1$, the continuity of $\varepsilon^{-1}dg/dx$ leads to

$$\begin{aligned}&\frac{1}{\varepsilon(x_p^-)}\left[c_7^{(p)}\, g(x_{p-1}) + \mathbf{c}_8^{(p)}\, \mathbf{g}_p + c_9^{(p)} g(x_p)\right]\\ &= \frac{1}{\varepsilon(x_p^+)}\left[c_1^{(p+1)}\, g(x_p) + \mathbf{c}_2^{(p+1)}\, \mathbf{g}_{p+1} + c_3^{(p+1)} g(x_{p+1})\right],\end{aligned} \tag{19}$$

where $\mathbf{g}_{p+1}$ is defined as $\mathbf{g}_p$ in (14), $c_1^{(p+1)}$, $\mathbf{c}_2^{(p+1)}$ and $c_3^{(p+1)}$ comprise the first row of $\mathbf{C}^{(p+1)}$ which is partitioned as $\mathbf{C}^{(p)}$ in (15). For $x_0 = 0$ and $x_P = L$, we impose the quasi-periodic condition (10) as

$$\begin{aligned}&\frac{e^{i\alpha_0 L}}{\varepsilon(x_0^+)}\left[c_1^{(1)}\, g(x_0) + \mathbf{c}_2^{(1)}\, \mathbf{g}_1 + c_3^{(1)} g(x_1)\right]\\ &= \frac{1}{\varepsilon(x_P^-)}\left[c_7^{(P)}\, g(x_{P-1}) + \mathbf{c}_8^{(P)}\, \mathbf{g}_P + c_9^{(P)} g(x_P)\right].\end{aligned} \tag{20}$$

From Eq. (19) for $1 \le p \le P-1$, Eq. (20) and the quasi-periodic condition (9), we can solve $g(x_0)$, $g(x_1)$, ..., $g(x_P)$ in terms of $\mathbf{g}_p$ for $1 \le p \le P$. We write down the result through a matrix $\mathbf{A}_0$ such that

$$\begin{bmatrix} g(x_0) \\ g(x_1) \\ \vdots \\ g(x_P) \end{bmatrix} = \mathbf{A}_0 \begin{bmatrix} \mathbf{g}_1 \\ \mathbf{g}_2 \\ \vdots \\ \mathbf{g}_P \end{bmatrix}. \tag{21}$$

Notice that $\mathbf{A}_0$ is a $(P+1) \times Q$ matrix, where $Q = (q_1 - 1) + (q_2 - 1) + ... = \sum_{p=1}^{P} q_p - P$ is the total number of interior discretization points.

On the pth segment, if we let $f = \varepsilon \partial_x(\varepsilon^{-1}\partial_x g)$, then f at the discrete points given in (12) can be approximately evaluated by a matrix $\mathbf{B}^{(p)}$, that is

$$\begin{bmatrix} f(x_{p-1}^+) \\ \mathbf{f}_p \\ f(x_p^-) \end{bmatrix} = \mathbf{B}^{(p)} \begin{bmatrix} g(x_{p-1}^+) \\ \mathbf{g}_p \\ g(x_p^-) \end{bmatrix}, \quad \mathbf{B}^{(p)} = \mathbf{E}^{(p)}\mathbf{C}^{(p)}[\mathbf{E}^{(p)}]^{-1}\mathbf{C}^{(p)},$$

where $\mathbf{f}_p$ is defined as $\mathbf{g}_p$ in (14), $\mathbf{E}^{(p)} = \mathrm{diag}[\varepsilon(\xi_{p0}^+), \varepsilon(\xi_{p1}), \varepsilon(\xi_{p2}), ..., \varepsilon(\xi_{p,q_p}^-)]$ is a diagonal matrix for ε evaluated at the discretization points. Similar to (15), we partition the matrix $\mathbf{B}^{(p)}$ as

$$\mathbf{B}^{(p)} = \begin{bmatrix} b_1^{(p)} & \mathbf{b}_2^{(p)} & b_3^{(p)} \\ \mathbf{b}_4^{(p)} & \mathbf{B}_5^{(p)} & \mathbf{b}_6^{(p)} \\ b_7^{(p)} & \mathbf{b}_8^{(p)} & b_9^{(p)} \end{bmatrix}. \tag{22}$$

The differential equation (8) is assumed to be valid at the interior discretization points of the segment, i.e., $\xi_{p,k}$ for $1 \le k < q_p$. This leads to

$$\left[\mathbf{B}_5^{(p)} + k_0^2 \mathbf{E}_s^{(p)} \mathbf{U}_s^{(p)}\right] \mathbf{g}_p + \mathbf{b}_4^{(p)} g(x_{p-1}) + \mathbf{b}_6^{(p)} g(x_p) = \beta^2 \mathbf{g}_p, \tag{23}$$

where $\mathbf{E}_s^{(p)} = \mathrm{diag}[\varepsilon(\xi_{p1}), \varepsilon(\xi_{p2}), ..., \varepsilon(\xi_{p,q_p-1})]$ is the central block of $\mathbf{E}^{(p)}$ and $\mathbf{U}_s^{(p)} = \mathrm{diag}[\mu(\xi_{p1}), \mu(\xi_{p2}), ..., \mu(\xi_{p,q_p-1})]$. Therefore, we have

$$\mathbf{A}_1 \begin{bmatrix} \mathbf{g}_1 \\ \mathbf{g}_2 \\ \vdots \\ \mathbf{g}_P \end{bmatrix} + \mathbf{A}_2 \begin{bmatrix} g(x_0) \\ g(x_1) \\ \vdots \\ g(x_P) \end{bmatrix} = \beta^2 \begin{bmatrix} \mathbf{g}_1 \\ \mathbf{g}_2 \\ \vdots \\ \mathbf{g}_P \end{bmatrix}, \tag{24}$$

where $\mathbf{A}_1$ is a block diagonal matrix with the pth diagonal block $\mathbf{B}_5^{(p)} + k_0^2 \mathbf{E}_s^{(p)} \mathbf{U}_s^{(p)}$, and

$$\mathbf{A}_2 = \begin{bmatrix} \mathbf{b}_4^{(1)} & \mathbf{b}_6^{(1)} & & & \\ & \mathbf{b}_4^{(2)} & \mathbf{b}_6^{(2)} & & \\ & & \ddots & \ddots & \\ & & & \mathbf{b}_4^{(P)} & \mathbf{b}_6^{(P)} \end{bmatrix}.$$

Combining (21) with the above equation, we obtain the following matrix eigenvalue problem

$$\mathbf{A} \begin{bmatrix} \mathbf{g}_1 \\ \mathbf{g}_2 \\ \vdots \\ \mathbf{g}_P \end{bmatrix} = \beta^2 \begin{bmatrix} \mathbf{g}_1 \\ \mathbf{g}_2 \\ \vdots \\ \mathbf{g}_P \end{bmatrix}, \tag{25}$$

where $\mathbf{A} = \mathbf{A}_1 + \mathbf{A}_2 \mathbf{A}_0$ is a $Q \times Q$ matrix. This leads to Q numerical eigenmodes. The eigenvector gives approximate values of g at the interior discretization points $\xi_{p,k}$ for $1 \leq k \leq q_p - 1$, but the values of g at the discontinuities x_p for $0 \leq p \leq P$, are also available from Eq. (21).

In the above formulation, a piecewise polynomial approximation to the eigenfunction is implicitly used through the differentiation matrix $\mathbf{C}^{(p)}$. The PEMM [22] explicitly uses polynomial approximations through expansions in Legendre or Chebyshev polynomials. The differential equation (8) is also approximated differently. We require that the equation is exactly valid at the interior discretization points, while PEMM requires expansion coefficients (except the last two) to vanish. However, the PEMM is only implemented for piecewise constant ε. Notice that if g is approximated by a polynomial but ε is not a constant on the segment, then $f = \varepsilon \partial_x (\varepsilon^{-1} \partial_x g)$ is not a polynomial in general. Of course, f can be further approximated by a polynomial, but the process becomes more complicated.

4. Interface conditions

Based on the pseudospectral method presented in the previous section, we can find Q_j numerical eigenmodes for the jth layer ($y_{j-1} < y < y_j$) by solving a $Q_j \times Q_j$ matrix eigenvalue

problem (25). The next step is to expand the field in each layer by the numerical eigenmodes and impose the interface conditions (11) between the layers approximately. The PSMM(p) [26] uses all Q_j numerical eigenmodes to expand the field in the jth layer, and then match u and $\varepsilon^{-1}\partial_y u$ at the interfaces between the layers by a point-matching scheme. Our approach is to use only a portion of the numerical eigenmodes in the field expansions and match the Fourier coefficients of u and $\varepsilon^{-1}\partial_y u$ at the interfaces.

Although the pseudospectral method exhibits exponential convergence, i.e., the errors decay exponentially as the number of discretization points is increased, not all numerical eigenmodes are accurate approximations of the true modes. In order to develop a numerical method which behaves more like the AMM, the numerical eigenmodes used in the expansions should be good approximations of the true modes. We use only N_j numerical eigenmodes in the eigenmode expansion (7), where N_j is about one half of Q_j or even less. The eigenmodes are ordered by the real part of the eigenvalue β^2. We denote the eigenmodes in the jth layer by $\{\beta_l^{(j)}, g_l^{(j)}\}$ for $1 \le l \le Q_j$ where $\mathrm{Re}[\beta_1^{(j)}]^2 \ge \mathrm{Re}[\beta_2^{(j)}]^2 \ge ...$, then the field in the jth layer is approximated by the following truncated eigenmode expansion:

$$u(x,y) \approx \sum_{l=1}^{N_j} \left\{ a_l^{(j)} \exp[i\beta_l^{(j)}(y - y_{j-1})] + b_l^{(j)} \exp[i\beta_l^{(j)}(y_j - y)] \right\} g_l^{(j)}(x), \tag{26}$$

where the eigenfunctions $g_l^{(j)}$ are actually only available at the discretization points given in (12).

To set up a system of equations for $\{a_l^{(j)}, b_l^{(j)}, R_m, T_m\}$, we need to impose the continuity conditions (11) at $y = y_0$, y_1, ..., y_J. If these conditions are imposed at all discretization points of x, we obtain an over-determined linear system which can be solved by the least squares method. We still call such a method point-matching pseudospectral modal method, since it is reduced to the PSMM(p) given in [26] when $N_j = Q_j$. Our preferred method is to match the Fourier coefficients as in the FMM. The two conditions (11) at $y = y_j$ are approximated by

$$\int_0^L \left[u(x, y_j^+) - u(x, y_j^-)\right] \exp(-i\alpha_m x) dx = 0, \tag{27}$$

$$\int_0^L \left[\frac{1}{\varepsilon(x, y_j^-)} \frac{\partial u}{\partial y}(x, y_j^-) - \frac{1}{\varepsilon(x, y_j^+)} \frac{\partial u}{\partial y}(x, y_j^+) \right] \exp(-i\alpha_m x) dx = 0 \tag{28}$$

for $-m_* \le m \le m_*$, where m_* is a positive integer and α_m is defined in (6). The total number of Fourier coefficients is $M = 2m_* + 1$. For $y = y_0^- = 0^-$, we use $u = u^{(t)}$ as given in

(5) and obtain

$$\int_0^L u(x,y_0^-)\exp(-i\alpha_m x) = LT_m, \tag{29}$$

$$\int_0^L \frac{1}{\varepsilon(x,y_0^-)}\frac{\partial u}{\partial y}(x,y_0^-)\exp(-i\alpha_m x) = -\frac{i\beta_m^{(0)}}{\varepsilon^{(0)}}LT_m. \tag{30}$$

For $y = y_J^+ = D^+$, we use $u = u^{(i)} + u^{(r)}$ as given in (3) and (4), and obtain

$$\int_0^L u(x,y_J^+)\exp(-i\alpha_m x) = L(R_m + \delta_{m0}), \tag{31}$$

$$\int_0^L \frac{1}{\varepsilon(x,y_J^+)}\frac{\partial u}{\partial y}(x,y_J^+)\exp(-i\alpha_m x) = -\frac{i\beta_m^{(*)}}{\varepsilon^{(*)}}L(R_m - \delta_{m0}), \tag{32}$$

where $\delta_{m0} = 1$ if $m = 0$ and $\delta_{m0} = 0$ if $m \neq 0$. In the jth layer, using the eigenmode expansion (26), the y-derivative of u is easily approximated as

$$\frac{\partial u}{\partial y}(x,y) \approx \sum_{l=1}^{N_j} i\beta_l^{(j)}\left\{a_l^{(j)}\exp[i\beta_l^{(j)}(y-y_{j-1})] - b_l^{(j)}\exp[i\beta_l^{(j)}(y_j-y)]\right\} g_l^{(j)}(x). \tag{33}$$

Therefore, we have

$$\int_0^L u(x,y_j^-)\exp(-i\alpha_m x)dx \approx \sum_{l=1}^{N_j} I_{lm}^{(j)}\left[a_l^{(j)}\gamma_l^{(j)} + b_l^{(j)}\right], \tag{34}$$

$$\int_0^L u(x,y_{j-1}^+)\exp(-i\alpha_m x)dx \approx \sum_{l=1}^{N_j} I_{lm}^{(j)}\left[a_l^{(j)} + b_l^{(j)}\gamma_l^{(j)}\right], \tag{35}$$

$$\int_0^L \frac{\partial_y u(x,y_j^-)}{\varepsilon(x,y_j^-)}\exp(-i\alpha_m x)dx \approx \sum_{l=1}^{N_j} J_{lm}^{(j)}\left[a_l^{(j)}\gamma_l^{(j)} - b_l^{(j)}\right], \tag{36}$$

$$\int_0^L \frac{\partial_y u(x,y_{j-1}^+)}{\varepsilon(x,y_{j-1}^+)}\exp(-i\alpha_m x)dx \approx \sum_{l=1}^{N_j} J_{lm}^{(j)}\left[a_l^{(j)} - b_l^{(j)}\gamma_l^{(j)}\right], \tag{37}$$

where

$$\gamma_l^{(j)} = \exp[i\beta_l^{(j)}(y_j - y_{j-1})], \tag{38}$$

$$I_{lm}^{(j)} = \int_0^L g_l^{(j)}(x)\exp(-i\alpha_m x)dx, \tag{39}$$

$$J_{lm}^{(j)} = i\beta_l^{(j)}\int_0^L \frac{g_l^{(j)}(x)}{\varepsilon^{(j)}(x)}\exp(-i\alpha_m x)dx. \tag{40}$$

The integrals $I_{lm}^{(j)}$ and $J_{lm}^{(j)}$ are evaluated in each segments by the Clenshaw-Curtis quadrature formulas [28] using exactly the discretization points given in (12).

Therefore, the conditions (27) and (28) lead to a linear system

$$\mathbf{F}\mathbf{z} = \mathbf{h}, \tag{41}$$

where

$$\mathbf{F} = \begin{bmatrix} \mathbf{F}_{00} & \mathbf{F}_{01} & & & \\ & \mathbf{F}_{11} & \mathbf{F}_{12} & & \\ & & \ddots & \ddots & \\ & & & \mathbf{F}_{JJ} & \mathbf{F}_{J,J+1} \end{bmatrix}, \quad \mathbf{z} = \begin{bmatrix} \mathbf{z}_0 \\ \mathbf{z}_1 \\ \vdots \\ \mathbf{z}_J \\ \mathbf{z}_{J+1} \end{bmatrix}, \quad \mathbf{h} = \begin{bmatrix} \mathbf{0} \\ \vdots \\ \mathbf{0} \\ \mathbf{h}_J \end{bmatrix}.$$

In the above, $\mathbf{z}_0$ and $\mathbf{z}_{J+1}$ are column vectors of length M for T_m and R_m ($|m| \le m_*$), respectively, $\mathbf{z}_j$ is column vector of length $2N_j$ for coefficients $a_l^{(j)}$ and $b_l^{(j)}$ ($1 \le l \le N_j$). The total length of $\mathbf{z}$ is $2M + 2\sum_{j=1}^{J} N_j$. Since we have imposed $2M$ conditions at each interface, the total number of equations in (41) is $2M(J+1)$. Each block in $\mathbf{F}$ and $\mathbf{h}$ has $2M$ rows. The right hand side $\mathbf{h}$ is only non-zero in the last block corresponding to the incident wave given in $y > y_J = D$. If we choose $N_j = M$ for $1 \le j \le J$, then $\mathbf{F}$ is a square matrix. However, in some cases, it is necessary to allow $N_j < M$, then (41) should be replaced by the least squares problem

$$\min_{\mathbf{z}} ||\mathbf{F}\mathbf{z} - \mathbf{h}||. \tag{42}$$

Furthermore, a constraint can be introduced to maintain the conservation of power as in [21]. In that case, the problem can be solved as a constrained least squares problem.

5. Numerical examples

In this section, we consider a number of examples including dielectric gratings and lossy or lossless metallic gratings. In all cases, we assume that the media are non-magnetic, thus $\mu = 1$. The first example has been previously analyzed by many authors. It is a metallic lamellar grating where the dielectric constant of the metal is $\varepsilon^{(0)} = (0.22 + 6.71i)^2$. The incident medium is air, thus $\varepsilon^{(*)} = 1$. The thickness and the period of the grating layer are $D = 1\,\mu$m and $L = 1\,\mu$m, respectively. In the grating layer, the dielectric constant is given by

$$\varepsilon(x) = \begin{cases} \varepsilon^{(*)}, & \text{if } 0 < x < 0.5L, \\ \varepsilon^{(0)}, & \text{if } 0.5L < x < L. \end{cases} \tag{43}$$

We consider a plane incident wave with an angle of incidence $\theta = 30^\circ$ and a free space wavelength $\lambda = 2\pi/k_0 = 1\,\mu$m.

For this example, we compare our PSMM(f) with the FMM and the PSMM(p). For the PSMM(f), we choose $N_1 = M$, where N_1 is the number of retained numerical eigenmodes in the eigenmode expansion (26) for the first and the only layer, and M is the total number

Fourier coefficients matched at the interfaces. For this choice, $\mathbf{F}$ is a square matrix. Since there is only one y-independent layer, i.e., $J = 1$, the size of $\mathbf{F}$ is $(4M)\times(4M)$. For computing the numerical eigenmodes, we set up a $Q_1 \times Q_1$ matrix $\mathbf{A}$ in (25), where Q_1 is larger than N_1. Since solving the matrix eigenvalue problem is the most time-consuming part of numerical modal methods, a fair comparison should have the same matrix sizes. Therefore, we compare our method with a FMM using Q_f Fourier modes where $Q_f \approx Q_1$. For the PSMM(p), the version that retains all Q_1 numerical eigenmodes in the expansions (i.e. $N_1 = Q_1$) does not give satisfactory results, especially for the TM case. As a result, we include only the PSMM(p) results obtained using $N_1 < Q_1$. For the TE polarization, we list the diffraction efficiency of the minus-first reflected order (RE_{-1}) obtained by the three methods in Table 1. It appears

Table 1. Example 1 (TE case): diffraction efficiency of the minus-first reflected order (RE_{-1}) calculated by the FMM, the PSMM(p) and the PSMM(f).

Q_f	FMM	Q_1	N_1	PSMM(p)	Q_1	N_1	PSMM(f)
41	0.73857	42	23	0.72240	42	23	0.7342706
81	0.73485	82	43	0.73323	82	43	0.7342804
121	0.73445	122	63	0.73401	122	63	0.7342792
161	0.73435	162	83	0.73418	162	83	0.7342790
201	0.73432	202	103	0.73423	202	103	0.7342789
241	0.73430	242	123	0.73425	242	123	0.7342789
281	0.73429	282	143	0.73426	282	143	0.7342789

that our method gives six accurate digits with $Q_1 = 122$ and $N_1 = 63$, while the FMM has three correct digits for $Q_f = 121$ and PSMM(p) has three correct digits for $Q_1 = 122$. A similar comparison for the TM polarization is given in Table 2, where approximate values of the diffraction efficiency of the zeroth reflected order (RE_0) are listed. For metallic gratings, the TM polarization is known to be more difficult to analyze. From Table 2, we observe that the PSMM(f) gives five correct digits (0.84848) for $Q_1 = 202$ and $N_1 = 103$, while the FMM still has only three correct digits with $Q_f = 401$ and PSMM(p) has only two correct digits for $Q_1 = 402$.

The second example is a dielectric lamellar grating previously studied by Lalanne and Hugonin [23]. The dielectric constants of the top and bottom media are $\varepsilon^{(*)} = 1$ (air) and $\varepsilon^{(0)} = 2.25$, respectively. The thickness and the period of the grating are $D = 1\,\mu$m and

Table 2. Example 1 (TM case): diffraction efficiency of the zeroth reflected order (RE_0) calculated by the FMM, the PSMM(p) and the PSMM(f).

Q_f	FMM	Q_1	N_1	PSMM(p)	Q_1	N_1	PSMM(f)
81	0.84677	82	43	0.84097	82	43	0.8481361
121	0.84752	122	63	0.84251	122	63	0.8484333
161	0.84784	162	83	0.84376	162	83	0.8484658
201	0.84802	202	103	0.84468	202	103	0.8484766
241	0.84813	242	123	0.84540	242	123	0.8484808
281	0.84819	282	143	0.84596	282	143	0.8484826
321	0.84823	322	163	0.84638	322	163	0.8484833
361	0.84825	362	183	0.84669	362	183	0.8484836
401	0.84827	402	203	0.84694	402	203	0.8484836

$L = 2\,\mu$m, respectively. In the grating layer, the dielectric constant satisfies

$$\varepsilon(x) = \begin{cases} 5.29, & \text{if } 0 < x < 0.234L, \\ 1, & \text{if } 0.234L < x < L. \end{cases}$$

As in the first example, we assume that the incident wave has a free space wavelength $\lambda = 1\,\mu$m and an incident angle $\theta = 30^\circ$. In Table 3, we show the diffraction efficiency of the

Table 3. Example 2 (TE case): diffraction efficiency of the zeroth transmitted order (TE_0) calculated by the FMM and the PSMM(f).

Q_f	FMM	Q_1	N_1	PSMM(f)
59	0.3661340	58	25	0.3661623
99	0.3661535	98	41	0.3661550
139	0.3661565	138	57	0.3661564
199	0.3661574	198	81	0.3661574
299	0.3661577	298	121	0.3661579
399	0.3661578	398	161	0.3661580

zeroth transmitted order (TE_0) obtained by the FMM and our method. The PSMM(f) results are obtained with $N_1 = M$, so that $\mathbf{F}$ is a square matrix. We observe that the performance of these two methods are nearly identical. For the TM case, if we choose $N_1 = M$, then

the PSMM(f) appears to be not as robust as the FMM. As N_1 and Q_1 are increased, the calculated diffraction efficiencies do not have smooth convergence behavior. Fortunately, this can be easily corrected by the least squares approach using $N_1 < M$. In Table 4, we show

Table 4. Example 2 (TM case): diffraction efficiency of the first transmitted order (TE_1) calculated by the FMM and the PSMM(f).

Q_f	FMM	Q_1	N_1	M	PSMM(f)
59	0.511053	58	25	31	0.511405
79	0.510829	78	33	41	0.511114
99	0.510730	98	41	51	0.510905
119	0.510676	118	49	61	0.510792
139	0.510652	138	57	71	0.510737
159	0.510637	158	65	81	0.510705
179	0.510625	178	73	91	0.510682
199	0.510618	198	81	101	0.510667
299	0.510603	298	121	151	0.510630
399	0.510598	398	161	201	0.510613
499	0.510596	498	201	251	0.510605

the results obtained by the PSMM(f) using an N_1 which is approximately 20% smaller than M. The results obtained by the FMM are also listed for comparison. It appears that the FMM results are slightly more accurate.

The third example is nearly identical to the first example, except that the metal is assumed to be lossless, so that $\varepsilon^{(0)} = -6.71^2$. We have the same geometric parameters ($L = D = 1\,\mu$m) and the same incident wave ($\lambda = 1\,\mu$m, $\theta = 30^\circ$). The dielectric constant of the grating layer is also given by (43), where $\varepsilon^{(*)} = 1$ and $\varepsilon^{(0)}$ is given above. In Table 5, we compare our results with those obtained by the FMM. For $Q_1 = 182$ and $N_1 = 93$, we obtain a result with six correct digits (0.848986), while the FMM result for $Q_f = 181$ has only four correct digits. For the TM case, the FMM is known to have a slow convergence [23]. In Fig. 1 and Table 6, we compare the diffraction efficiencies of the zeroth reflected order obtained by our method and the FMM. For $Q_1 = 262$ and $N_1 = 133$, the PSMM(f) gives 5 correct digits (0.89298), while FMM has only three correct digits for $Q_f = 401$. The PSMM(f) results for this examples are obtained with $N_1 = M$.

The fourth example was recently analyzed by Gundu and Mafi [20, 21]. The dielectric constants of the top and bottom media are $\varepsilon^{(*)} = 2.25$ and $\varepsilon^{(0)} = 1.69$, respectively. The thickness and the period of the grating layer are $D = 0.28\,\mu$m and $L = 0.2\,\mu$m, respectively.

Table 5. Example 3 (TE case): diffraction efficiency of the minus-first reflected order (RE_{-1}) calculated by the FMM and the PSMM(f).

Q_f	FMM	Q_1	N_1	PSMM(f)
41	0.85450	42	23	0.8489010
61	0.85070	62	33	0.8489542
81	0.84972	82	43	0.8489807
101	0.84936	102	53	0.8489846
141	0.84912	142	73	0.8489854
181	0.84905	182	93	0.8489856
241	0.84901	242	123	0.8489857
301	0.84899	302	153	0.8489858

Table 6. Example 3 (TM case): diffraction efficiency of the zeroth reflected order (RE_0) calculated by the FMM and the PSMM(f).

Q_f	FMM	Q_1	N_1	PSMM(f)
61	0.8924	62	33	0.892132
101	0.8896	102	53	0.892879
141	0.8938	142	73	0.892946
181	0.8916	182	93	0.892967
261	0.8929	262	133	0.892978
401	0.8928	402	203	0.892980

In the grating layer, the dielectric function is given by

$$\varepsilon(x) = \begin{cases} -2.5, & \text{if } 0 < x < 0.5L, \\ 1.69, & \text{if } 0.5L < x < L. \end{cases}$$

We consider a normal incident wave ($\theta = 0^\circ$) with a free space wavelength $\lambda = 0.62\,\mu$m for the TM polarization. In [20], it is shown that the standard FMM and even the AMM have convergence difficulties for this problem, and the least squares approach is proposed to solve the problem. To maintain power balance, a constrained least squares approach is developed in [21]. In Fig. 2(a), we show the diffraction efficiency of the zeroth reflected order calculated by the standard FMM. As shown in Fig. 2(b), the convergence problem also appears in the PSMM(f) if we choose $N_1 = M$. Fortunately, the least squares and constrained least squares

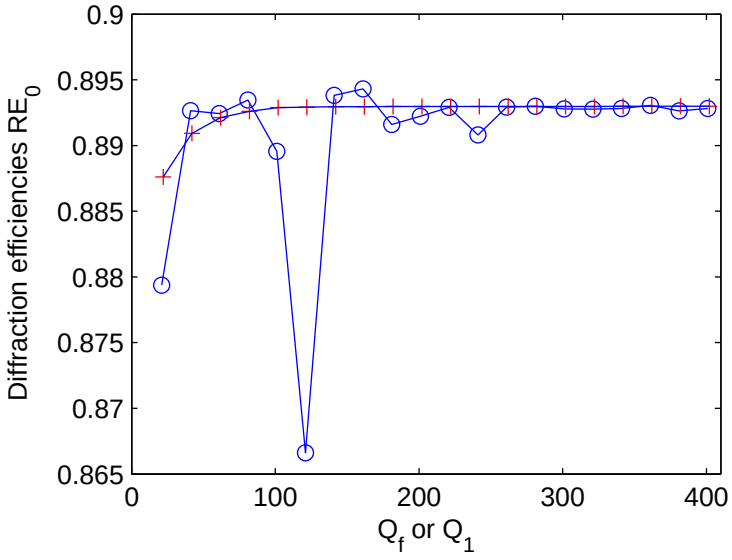

Fig. 1. Example 3 (TM case): diffraction efficiency of the zeroth reflected order calculated by the FMM (circles) and the PSMM(f) (pluses).

approaches can also be used with the PSMM(f) to produce reliable solutions. In Fig. 2 and Table 7, we show the diffraction efficiency of the zeroth reflected order calculated by the PSMM(f) with $N_1 = (M+1)/2$. The normalized total power of the scattered field is also shown and it is exactly one. However, the convergence is rather slow.

6. Conclusion

In the previous sections, a Fourier-matching pseudospectral modal method is developed for lamellar diffraction gratings or lamellar grating stacks (with uniform, i.e. y-independent, layers). Our objective is to develop a method which calculates the eigenmodes more accurately and performs more like the analytic modal method. We use a Chebyshev pseudospectral method to calculate the eigenmodes in each y-independent layer. Unlike the point-matching pseudospectral method developed in [26], we match the Fourier coefficients at interfaces between the layers. Furthermore, not all numerical eigenmodes are used to expand the field in the uniform layers, since some of these modes do not approximate the true eigenmodes. Finally, the least squares and constrained least squares approach developed for the Fourier modal method by Gundu and Mafi [20, 21] are also incorporated into our method.

Compared with the standard version of the Fourier modal method [14–16], our method performs better except for a case involving a dielectric grating. For highly conductive gratings and when the constrained least squares approach is used, our method may still have a very

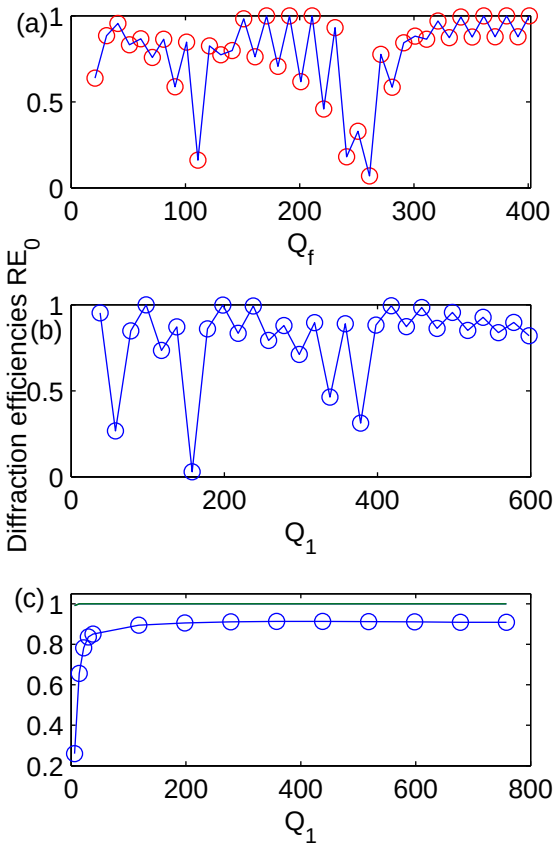

Fig. 2. Example 4 (TM case): diffraction efficiency of the zeroth reflected order calculated by (a) the FMM, (b) the PSMM(f) with $N_1 = M$, (c) the PSMM(f) with $N_1 = (M + 1)/2$.

slow convergence, but this appears to be a common problem for all modal methods. We notice that the Fourier modal method has been improved by the adaptive spatial resolution technique [17]. It is likely that a similar technique can be developed for the pseudospectral modal method.

Acknowledgments

This research was partially supported by a grant from the Research Grants Council of Hong Kong Special Administrative Region, China (Project No. CityU 102008).

Table 7. Example 4 (TM case): diffraction efficiencies of the zeroth reflected order by the PSMM(f).

Q_1	M	N_1	RE_0
118	61	31	0.8950
198	101	51	0.9058
278	141	71	0.9114
358	181	91	0.9133
438	221	111	0.9138
518	261	131	0.9119
598	301	151	0.9109
678	341	171	0.9094
758	381	191	0.9088

References

1. L. C. Botten, M. S. Craig, R. C. McPhedran, J. L. Adams, and J. R. Andrewartha, "The dielectric lamellar diffraction grating," Optica Acta **28**, 413-428 (1981).
2. L. C. Botten, M. S. Craig, R. C. McPhedran, J. L. Adams, and J. R. Andrewartha, "The finitely conducting lamellar diffraction grating," Optica Acta **28**, 1087-1102 (1981).
3. L. C. Botten, M. S. Craig, and R. C. McPhedran, "Highly conducting lamellar diffraction gratings," Optica Acta **28**, 1103-1106 (1981).
4. P. Sheng, R. S. Stepleman, and P. N. Sanda, "Exact eigenfunctions for square wave gratings — application to diffraction and surface-plasmon calculations," Phys. Rev. B **26**, 2907-2916 (1982).
5. A. Roberts and R. C. McPhedran, "Power losses in highly conducting lamellar gratings," J. Mod. Opt. **34**, 511-538 (1987).
6. L. Li, "A modal analysis of lamellar diffraction gratings in cornical mountings," J. Mod. Opt. **40**, 553-573 (1993).
7. L. Li, "Multilayer modal method for diffration gratings of arbitrary profile, depth, and permittivity," J. Opt. Soc. Am. A **10**, 2581-2591 (1993).
8. J. M. Miller, J. Turunen, E. Noponen, A. Vasara, and M. R. Taghizadeh, "Rigorous modal theory for multiply grooved lamellar gratings," Opt. Commun. **111**, 526-535 (1994).
9. M. Foresti, L. Menez, and A. V. Tishchenko, "Modal method in deep metal-dielectric gratings: the decisive role of hidden modes," J. Opt. Soc. Am. A **23**, 2501-2509 (2006).

10. S. Campbell, L. C. Botten, R. C. McPhedran, and C. M. de Sterke, "Modal method for classical diffraction by slanted lamellar gratings," J. Opt. Soc. Am. A **25**, 2415-2426 (2008).
11. C. B. Burckhardt, "Diffraction of a plane wave at a sinusoidally stratified dielectric grating," J. Opt. Soc. Am. **56**, 1502-1509 (1966).
12. K. Knop, "Rigorous diffraction theory for transmission phase gratings with deep rectangular grooves," J. Opt. Soc. Am. **68**, 1206-1210 (1978).
13. M. G. Moharam and T. K. Gaylord, "Diffraction analysis of dielectric surface-relief gratings," J. Opt. Soc. Am. **72**, 1385-1392 (1982).
14. P. Lalanne and G. M. Morris, "Highly improved convergence of the coupled-wave method for TM polarization," J. Opt. Soc. Am. A **13**, 779-784 (1996).
15. G. Granet and B. Guizal, "Efficient implementation of the coupled-wave method for metallic lamellar gratings in TM polarization," J. Opt. Soc. Am. A **13**, 1019-1023 (1996).
16. L. Li, "Use of Fourier series in the analysis of discontinuous periodic structures," J. Opt. Soc. Am. A **13**, 1870-1876 (1996).
17. G. Granet, "Reformulation of the lamellar grating problem through the concept of adaptive spatial resolution," J. Opt. Soc. Am. A **16**, 2510-2516 (1999).
18. N. M. Lyndin, O. Parriaux, and A. V. Tishchenko, "Modal analysis and suppression of the Fourier modal method instabilities in highly conductive gratings," J. Opt. Soc. Am. A **24**, 3781-3788 (2007).
19. I. Gushchin and A. V. Tishchenko, "Fourier modal method for relief gratings with oblique boundary conditions," J. Opt. Soc. Am. A **27**, 1575-1583 (2010).
20. K. M. Gundu and A. Mafi, "Reliable computation of scattering from metallic binary gratings using Fourier-based modal methods," J. Opt. Soc. Am. A **27**, 1694-1700 (2010).
21. K. M. Gundu and A. Mafi, "Constrained least squares Fourier modal method for computing scattering from metallic binary gratings," J. Opt. Soc. Am. A **27**, 2375-2380 (2010).
22. R. H. Morf, "Exponentially convergent and numerically efficient solution of Maxwell's equations for lamellar gratings," J. Opt. Soc. Am. A **12**, 1043-1056 (1995).
23. P. Lalanne and J. P. Hugonin, "Numerical performance of finite-difference modal methods for the electromagnetic analysis of one-dimensional lamellar gratings," J. Opt. Soc. Am. A **17**, 1033-1042 (2000).
24. K. Edee, P. Schiavone, and G. Granet, "Analysis of defect in extreme UV lithography mask using a modal method based on nodal B-spline expansion," Japanese Journal of Applied Physics, Part 1 **44**, 6458-6462 (2005).
25. G. Granet, L. B. Andriamanampisoa, K. Raniriharinosy, A. M. Armeanu, and K. Edee,

"Modal analysis of lamellar gratings using the moment method with subsectional basis and adaptive spatial resolution," J. Opt. Soc. Am. A **27**, 1303-1310 (2010).

26. Y.-P. Chiou, W.-L. Yeh, and N.-Y. Shih, "Analysis of highly conducting lamellar gratings with multidomain pseudospectral method," J. Lightwave Technol. **27**, 5151-5159 (2009).
27. L. N. Trefethen, *Spectral Methods in MATLAB*, (Society for Industrial and Applied Mathematics, 2000).
28. L. N. Trefethen, "Is Gauss quadrature better than Clenshaw-Curtis?", SIAM Review **50**, 67-87 (2008).